A&A 418, 177–184 (2004)
DOI: 10.1051/0004-6361:20034331

Astronomy & Astrophysics

Spatially and spectrally resolved 10 μm emission in Herbig Ae/Be stars*

R. van Boekel[1,2], L. B. F. M. Waters[1,3], C. Dominik[1], C. P. Dullemond[4], A. G. G. M. Tielens[5], and A. de Koter[1]

[1] Astronomical Institute "Anton Pannekoek", University of Amsterdam, Kruislaan 403, 1098 SJ Amsterdam, The Netherlands
[2] European Southern Observatory, Karl-Schwarzschildstrasse 2, 85748 Garching bei München, Germany
[3] Instituut voor Sterrenkunde, Katholieke Universiteit Leuven, Celestijnenlaan 200B, 3001 Heverlee, Belgium
[4] Max-Planck-Institut für Astrophysik, Karl-Schwarzschildstrasse 1, Postfach 1317, 85748 Garching bei München, Germany
[5] Kapteyn Astronomical Institute, PO Box 800, 9700 AV Groningen, The Netherlands

Received 17 September 2003 / Accepted 23 January 2004

Abstract. We present new mid-infrared spectroscopy of the emission from warm circumstellar dust grains in the Herbig Ae stars HD 100546, HD 97048 and HD 104237, with a spatial resolution of $\approx 0\farcs9$. We find that the emission in the *UIR* bands at 8.6, 11.3 and (HD 97048 only) 12.7 μm is extended in the first two sources. The continuum emission is resolved in HD 97048 and possibly in HD 100546. HD 104237 is not spatially resolved in our observations. We find that the *UIR* emission in HD 100546 and HD 97048 is extended on a scale of (several) 100 AU, corresponding to the outer disk scale in flaring disk models. Small carbonaceous particles are the dominant source of opacity in the HD 97048 disk.

Key words. circumstellar matter – stars: pre-main sequence – infrared: ISM – ISM: lines and bands

1. Introduction

Herbig Ae/Be stars (HAEBEs, Herbig 1960) are intermediate mass pre-main-sequence stars surrounded by material which is left from the star formation process. A sub-group of mostly late B and A-F type HAEBE stars (hereafter HAEs) show little or no optical extinction and usually low mass accretion rates, as derived from radio analysis (Skinner et al. 1993) and the lack of significant veiling in optical spectra. The spatial distribution of the circumstellar material of these HAEs is a matter of debate. While the millimeter emission observed from some stars originates from a compact dust disk which appears to be keplerian (Mannings & Sargent 1997), near-IR interferometric observations seem consistent with the hottest dust having a more spherical distribution (Millan-Gabet et al. 2001). Only recently very high resolution interferometric measurements at 2.2 μm have provided strong evidence for non-circular symmetry on sub-AU scales, indicating disk like geometries in the innermost regions of HAE systems (Eisner et al. 2003). Optical and near-infrared images in scattered light argue for disk geometries on large scales of 100 AU (Grady et al. 2001; Augereau et al. 2001). Thus, evidence is growing that HAE stars indeed have disks.

The mid-infrared spectra of HAEs are dominated by a strong continuum caused by warm grains in the immediate vicinity of the star, and solid state emission bands from silicates and carbonaceous material (Meeus et al. 2001a; Natta et al. 2001). The IR emission is believed to originate mostly from the surface layer of a passively heated dusty disk (Chiang & Goldreich 1997). Indeed, recent hydrostatic disk models are successful in explaining the spectra of HAEs in the context of such disk models, without requiring other spatial components, such as a spherical halo (Dullemond et al. 2001).

The location of the dust and the dust opacities determine the structure and emission properties of the disk. Direct studies of the inner disk structure require interferometric measurements. On larger spatial scales, where we can probe the outermost regions of the disk using single telescopes, the blackbody temperatures are much too low for significant 10 μm emission to be produced. Such 10 μm emission could only arise from a population of very small "super-heated" grains (VSG), and emission from large carbonaceous molecules (Polycyclic Aromatic Hydrocarbons, or PAHs) that can be excited by single photon absorption. If present in the outer disk, these molecules offer a unique probe of the outer disk structure since they can radiate at all stello-centric distances, irrespective of the local blackbody temperature.

Meeus et al. (2001b) noted that based on the IR Spectral Energy Distribution (SED), HAEs can be divided into two main

Send offprint requests to: R. van Boekel,
e-mail: vboekel@science.uva.nl

* Based on observations obtained at the European Southern Observatory (ESO), La Silla, and on observations with ISO, an ESA project with instruments funded by ESA Member States (especially the PI countries: France, Germany, The Netherlands and the UK) and with the participation of ISAS and NASA.

groups: group I sources that have a very strong, rising IR excess peaking around 60 μm, and group II sources displaying a more moderate and less steeply rising IR excess. In the disk hypothesis, group I sources show a flaring outer disk geometry, such that the disk can intercept and re-process stellar radiation out to large stello-centric radii. In group II sources, the outer disk is not flaring, leading to lower temperatures. It is therefore expected that group I sources will show more extended emission and the disk emission in group II sources will be concentrated close to the central star.

A critical test of disk models requires high angular resolution observations at IR and millimeter wavelengths. Mid-infrared imaging using single-dish telescopes has shown that several HAEs are extended on a scale of 0.5 to 2 arcsec, corresponding to about 100 AU (Grady et al. 2001; Fischer et al. 2000; Jayawardhana et al. 2001; Ressler & Barsony 2003).

Long slit spectroscopy is ideally suited for detecting spatially resolved structures emitting in narrow spectral regions (i.e. emission lines/bands), when observing close to the resolution limit. The profile of the spectrum in the spatial direction is measured *instantaneously* in the emission band and in the continuum next to it. Therefore, a *relative* increase in size can be detected with high confidence, even if the response of the telescope to a point source (the point spread function, PSF) is not known accurately. However, a long-slit spectrum yields spatial information only along the direction of the slit.

Here, we report on spatially and spectrally resolved mid-IR observations observations of three HAE stars, HD 97048, HD 100546 (both group I), and HD 104237 (group II). Both group I stars show prominent emission in the Unidentified InfraRed (*UIR*) bands (Aitken & Roche 1981; Waelkens et al. 1996), usually attributed to PAHs. HD 97048 is in a reflection nebula and has been shown to have extended mid-IR emission from *UIR* bands (e.g. Siebenmorgen et al. 2000) on a scale of about 10 arcsec.

2. Observations and data reduction

Long slit infrared spectra in the 10 μm atmospheric window were taken on 27 December 2001 and 19 March 2003 with the *Thermal Infrared Multi Mode Instrument 2* (TIMMI2, Reimann et al. 1998), mounted at the 3.60 m telescope at the ESO La Silla observatory. We used the low resolution ($R \approx 160$) N band grism and a slit width of 1.2 arcsec, the pixel scale in the spectroscopic mode of TIMMI2 is 0.45 arcsec. To correct for the strong atmospheric and instrumental background at 10 μm, we employed chopping and nodding, using a $+10''$ chop throw north-south, and a $-10''$ nod throw north-south. This renders us insensitive to diffuse emission on scales larger than $5''$. Spectroscopic standard stars were observed regularly and were used to correct for the non-uniform atmospheric transmission. A summary of the observations is given in Table 1.

The (absolute) photometric accuracy of our observations is about 15%. In order to faciliate the comparison of the TIMMI 2 spectra and ISO-SWS spectra, simple scaling factors ($\approx$1) have been applied to the TIMMI 2 spectra, such as to give the best match with ISO (note that the absolute accuracy of ISO is about the same as that of our TIMMI 2 data).

Table 1. Summary of the observations. The fourth column lists the seeing at 0.5 μm as measured by the DIMM monitor. Distances are calculated from Hipparcos parallaxes.

Object	UT	AM	Seeing	d [pc]
26 December 2001:				
HD 81797	7:09	1.08	0.″57	
HD 100546	7:25	1.42	0.″76	103^{+7}_{-6}
HD 104237	7:51	1.60	0.″84	116^{+8}_{-7}
HD 81797	8:50	1.12	0.″70	
19 March 2003:				
HD 55865	2:23	1.46	0.″94	
HD 97048	3:02	1.51	0.″93	175^{+27}_{-21}
HD 63295	3:33	1.55	0.″93	

3. Analysis of the spatial profiles

The resolution of our long slit spectra in the spatial direction is limited by diffraction, atmospheric perturbations of the wavefront ("seeing"), abberations due to imperfect telescope optics, and the sampling of the signal by the detector. At 10 μm, our observations are close to the diffraction limit, though the degradation of the PSF caused by the atmosphere is non-negligible. The 0.″45 pixel size causes our spectra to be undersampled in the spatial direction. This hampers size estimates of objects that are only marginally resolved, i.e. less than $1''$ in size, since the spatial profiles of science target and PSF reference star will depend on the exact positioning of the object on the detector pixels (a star positioned in the center of a pixel will yield a significantly different spatial profile from a star that is on the edge of a pixel). This problem can be overcome by fitting Gaussians to the spatial profiles of science star and PSF reference, instead of comparing them directly. The fitted *FWHM* is hardly sensitive to differences in positioning. The drawback of this approach is that our measured PSF deviates somewhat from the Gaussian shape in its wings. Therefore, the spatial extent of an extended emission component that is present along with a more compact component cannot be accurately determined if the relative flux contribution of the former component is low.

3.1. Determination of the PSF

When estimating the PSF during the observations of the science targets, we approximate the various contributions to the PSF by Gaussians. In order to quantify the seeing contribution, we compute the expected PSF using a geometrical model for the telescope, and a simulation code for atmospheric turbulence (Conan et al. 2003) which requires the seeing (s) as an input parameter. The seeing at La Silla is monitored by a DIMM (Sandrock et al. 2000) and we use these measurements. This yields the (square of the) width of the synthetic PSF, $\sigma^2_{\rm PSF,syn}(\lambda)$, which is compared to the actual observed PSF, $\sigma^2_{\rm PSF,obs}(\lambda)$. The abberations from the telescope optics are then computed as $\sigma^2_{\rm abb}(\lambda) = \sigma^2_{\rm PSF,obs}(\lambda) - \sigma^2_{\rm PSF,syn}(\lambda)$. Since the science object is generally observed at a different

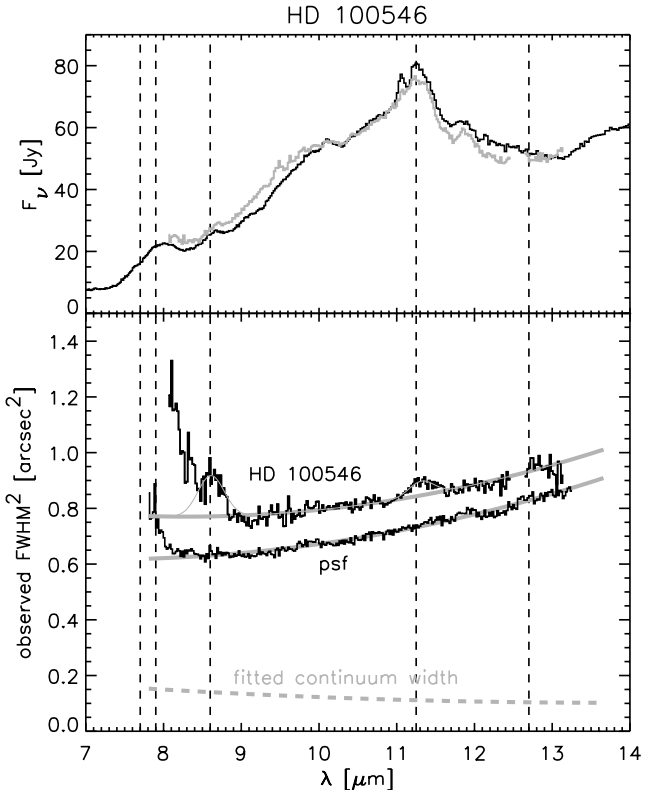

Fig. 1. $FWHM^2$ of the spatial profile as a function of wavelength of HD 100546 and the model PSF (*lower panel*). The solid grey curves show polynomial fits to the $FWHM^2$ of the PSF and the continuum (i.e. the emission outside the *UIR* bands). The fitted continuum width is indicated with the dashed grey curve. The vertical dashed lines indicate the wavelengths of the *UIR* bands. The *upper panel* shows the ISO SWS spectrum of HD 100546 in black and the ground based spectrum in grey.

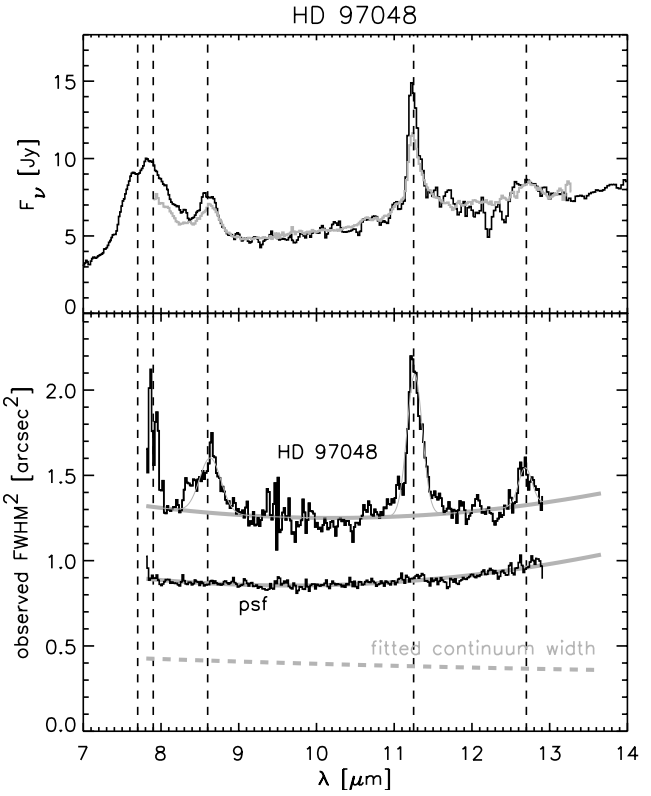

Fig. 2. $FWHM^2$ of the spatial profile as a function of wavelength of HD 97048 and the observed psf (*lower panel*). The solid grey curves show polynomial fits to the $FWHM^2$ of the PSF and the continuum (i.e. the emission outside the *UIR* bands). The fitted continuum width is indicated with the dashed grey curve. The vertical dashed lines indicate the wavelengths of the *UIR* bands. The *upper panel* shows the ISO SWS spectrum of HD 97048 in black and the ground based spectrum in grey.

airmass and under different seeing conditions than the PSF reference, we compute the synthetic PSF for the airmass and seeing of the science observation, and obtain the PSF of the science measurement as $\sigma^2_{\rm PSF,sci}(\lambda) = \sigma^2_{\rm sci,syn}(\lambda) + \sigma^2_{\rm abb}(\lambda)$. When $\sigma_{\rm PSF,sci}$ is calculated for all wavelengths, we fit a second order polynomial to $\sigma^2_{\rm PSF,sci}(\lambda)$ which is our final PSF. In Figs. 1–3, the PSF and the polynomial fit to it are labeled "PSF", and are shown in black and grey, respectively. The *FWHM* of the calibration star profiles show an unexplained increase with respect to the expected behaviour between 8 μm and the atmospheric cut-off at $\approx$7.8 μm. Therefore we must be careful when interpreting the profiles of the science targets in this wavelength range.

We use this method to determine the PSF during the observations of HD 100546 and HD 104237. The method assumes that the static abberations due to the telescope optics are independent of telescope elevation. Unfortunately, no measurement of a calibration star is available at airmasses comparable to the HD 100546 and HD 104237 measurements. However, the spatial profile measured in our observation of HD 104237 agrees very well with the predicted PSF. If the spatial extent of HD 104237 is $\ll 1''$ (as one may expect, based on modeling of its SED, and the non-detection in scattered light images (Danks et al. 2001), contrary to HD 100546 and several other group I HAe stars (Pantin et al. 2000, Grady et al. 2001) this measurement shows that our assumptions are valid. Note that HD 97048 which, according to the SED and the spatially resolved data in this work, should show extended structure in scattered light images, has not yet been observed in this fashion. The calibration stars used for the HD 97048 were taken just before and after the science measurement, at nearly identical airmass and under indentical seeing conditions, and we have therefore a direct determination of the PSF.

4. Spatially extended emission

4.1. HD 100546

The measured $FWHM(\lambda)$ of the spatial profile of HD 100546 and the predicted PSF during this measurement are shown in the lower panel of Fig. 1. The source appears to be marginally resolved in the continuum, and a small but significant increase in size is seen in the *UIR* bands at 8.6 and 11.3 μm, and shortward of 8.4 μm. We assume a Gaussian profile for the continuum emission and derive a *FWHM* of 30 ± 30 AU. The continuum appears only marginally resolved but we note that the estimated size of the continuum agrees well with the size

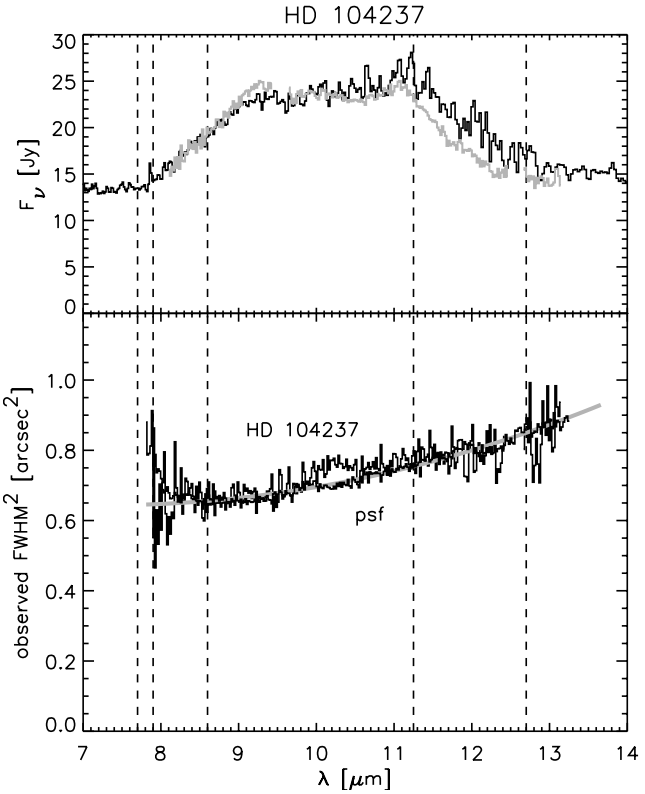

Fig. 3. *FWHM*^{2} of the spatial profile as a function of wavelength of HD 104237 and the model PSF (*lower panel*). The solid grey curve shows a polynomial fit to the *FWHM*^{2} of the PSF. The vertical dashed lines indicate the wavelengths of the *UIR* bands. The *upper panel* shows the ISO SWS spectrum of HD 104237 in black and the ground based spectrum in grey.

estimated from the SED by Bouwman et al. (2003). The derived size also agrees with the size derived by Liu et al. (2003), who find a *FWHM* of 24 AU in a recent nulling experiment on a 6.5m telescope. Using the residual (total minus silicate emission) spectra of Bouwman et al. (2003), we estimate the contribution of the *UIR* bands to the total flux to be approximately 22% and 13% at 8.6 and 11.3 μm, respectively. We deduce *FWHM* values of 140 ± 50 AU and 150 ± 100 AU for the 8.6 and 11.3 μm *UIR* bands, using the expected PSF and assuming that also the *UIR* emission has a Gaussian light distribution. Note that the spatially extended *UIR* emission at these wavelengths contributes only a relatively minor fraction to the total flux. Therefore, an accurate determination of the sizes of the emitting regions is not possible, which is reflected in the relatively large error bars on the estimates quoted above. However, the increase in spatial extent in the *UIR* bands is seen at the wavelengths of *all* the *UIR* features, and the conclusion that the *UIR* emission is more extended than the continuum emission is therefore unavoidable. In an absolute sense, the size of *UIR* the emitting region *must* be of order 100 AU in order for it to be resolved by our 3.6 m telescope.

Grady et al. (2001) (hereafter GR01) find evidence for extended emission at 11.7 μm using a narrow-band filter, which they attribute to either UIBs or silicates. We show here that the extended emission is in fact due to UIBs. The measured *FWHM* in the GR01 image is 1.″03, slightly larger than the mean *FWHM* in the spatial direction of our longslit spectrum in the passband of the 11.7 μm filter, which is 0.″94. GR01 find that over the whole *N*-band the source is essentially unresolved, which is consistent with our findings: if the spatial extent that is tentatively detected here is real, an observation at an 8 m class telescope would be needed to make a solid detection.

Due to the atmospheric cut-off at ≈7.8 μm we only see the red wing of the strong 7.7 μm *UIR* band. Even though the PSF is not fully understood here, the very strong rise in *FWHM* shortward of 8.4 μm indicates that also the *UIR* emission here is resolved in our data. Assuming a PSF *FWHM* of 0.″95 and an *UIR* contribution of 65%, a rough estimate of the *UIR FWHM* in the 7.7–7.9 μm complex yields a value of 140 AU. Since conditions did not allow measurements at wavelengths shortward of 8.0 micron, this estimate involves extrapolation of the profile, adding considerable uncertainty. We note however, that the derived size is consistent with the values measured in the 8.6 and 11.3 μm bands.

Despite the strong silicate emission that has significant spectral sub-structure due to crystalline material, we see no wavelength dependence of the *FWHM* outside the *UIR* emission bands. The emission from both the crystalline and amorphous silicates must arise from a physically much smaller region than the *UIR* emission.

4.2. HD 97048

The spectrum of HD 97048 in the 10 μm range is dominated by *UIR* emission (Gürtler et al. 1999; Siebenmorgen et al. 2000, hereafter SI00). There is no evidence for a silicate emission band. As can be seen in Fig. 2, the spatial extent of this source in the continuum emission is significantly higher than that of the measured PSF. In the *UIR* bands at 8.6, 11.3 and 12.7 μm the *FWHM* shows clear peaks indicating that the feature emission is still more extended.

Assuming a Gaussian light distribution for both the continuum and *UIR* feature emission, we deduce a *FWHM* of 110 ± 40 AU for the continuum emission at 10.5 μm, and *FWHM* values of 210 ± 70, 270 ± 70 and 290 ± 100 AU for the 8.6 11.3 and 12.7 μm *UIR* bands, respectively. We estimate the contribution of the 8.6, 11.3 and 12.7 μm *UIR* bands to the total flux to be 44%, 59% and 16%.

Previous studies already showed that the mid-IR emission in HD 97048 is extended (Prusti et al. 1994, SI01) on a scale of 5–10 arcsec, and this was attributed to emission in the *UIR* bands. We are insensitive to diffuse emission on these scales but with our higher spatial resolution we resolve the emission from the central source. Possibly, we have resolved the emission from a large, flared disk, whereas the extended emission seen by SI00 originates in the loose surroundings.

In our interpretation of the SED of HD 97048, namely that it is a passive, flaring disk, the outer disk needs to have opacity both at optical/UV wavelengths (to absorb the stellar radiation) and infrared wavelengths (to emit the observed 10 μm continuum radiation). The spatial extent of the continuum emission implies that the grain population dominating the continuum is

not in thermal equilibrium. The blackbody temperature at a distance of 50 AU from the central star is about 100 K, too low for significant emission in the 10 μm region. The continuum must be dominated by very small "superheated" grains. HD 97048 has no silicate feature and therefore it is excluded that silicates are the source of the continuum. As the grains producing the continuum radiation are necessarily small, they would show a very strong emission band, peaking around 9.7 μm, *if* they would consist of silicate material. For a continuum opacity source small carbonaceous particles are the most likely candidate. Carbon has a high opacity both in the optical and at 10 μm. We note that metallic iron nano-particles also show no spectral structure and thus may be responsible for the observed extended emission. However, the strong *UIR* bands suggest a prominent population of small carbon rich particles is likely present. Thus, carbon appears to dominate the opacity of Herbig star disks if no silicates are present. In sources where small silicate grains are seen in the spectrum, carbonaceous material may also be responsible for a significant fraction of the opacity, along with the silicates.

4.3. HD 104237

The group II source HD 104237 is shown in Fig. 3. The measured spatial profile is identical to that of the expected PSF. The increase in *FWHM* at 10.0–10.4 μm is not confirmed by a repeated observation in march 2003 and remains unexplained. We conclude that HD 104237 is unresolved in our observations, and that the bulk of the 10 μm emission in this source must arise from a region $\leq$30 AU in diameter. Though this is consistent with the idea that group II sources do not posess a flaring outer disk, this measurement does not put stringent requirements on models for group II disks. Higher spatial resolution observations are needed to critically test theory.

5. Discussion

5.1. The 7.7–8.6 μm region

In HD 97048, both the 7.7-7.9 μm and the 8.6 μm band are very prominent. With respect to "normal" PAHs, as found in the ISM, HD 97048 has excess emission at 8.0–8.2 μm (Peeters et al. 2002). The spatial extent of this excess emission does not appear significantly larger than that of the continuum emission (Fig. 2), whereas the emission in the 7.7–7.9 μm and the 8.6 μm band is spatially more extended. This indicates that the properties of the carrier of the 8.0–8.2 μm excess emission are different from those of the carriers of the "normal" PAH bands.

Also HD 100546 has excess emission around 8.2 μm compared to the PAH spectrum as observed in the ISM. It can be seen in Fig. 1 that as we trace the spatial extent of the emission blue-ward of the peak of the 8.6 μm feature, after an initial drop, the *FWHM* starts to increase again at 8.4 μm (in HD 97048 this happens only at 8.1 μm), indicating that the excess emission is spatially extended on a scale of approximately 100 AU. The carrier of this band must therefore a very small, non-thermal equilibrium grain. Possibly, it is a processed PAH molecule, larger than a typical ISM PAH. Our data suggest that the 8.2 μm excess emission originates predominantly from the central source rather than the surrounding nebula (see also Sect. 5.2).

The reason we observe the excess emission at 8.2 μm to be much more extended than the continuum in HD 100546, whereas in HD 97048 this is not obviously so, is likely a matter of contrast. In HD 100546, the continuum is dominated by silicates, which do not emit much at 8.2 μm (and emit significantly in the 10 μm window only within about 15 AU from the star). The 8.2 μm emission in this star is fully dominated by the PAHs. In HD 97048 the continuum emission at 8.2 μm dominates the total flux. It arises from small carbonaceous grains and the continuum emission has a *FWHM* of about 100 AU, equal within errors to the *FWHM* of the 8.2 μm excess emission in HD 100546. It is therefore not surprising that we observe the 8.2 μm excess emission in HD 97048 not to be significantly more extended than the continuum, contrary to HD 100546.

5.2. PAH energetics

The maximum size a PAH molecule (or VSG) can have in order to emit significantly in the 10 μm region, depends on the ambient radiation field. The smallest particles can be heated to several hundred K upon absorption of a single photon and can thus radiate 10 μm emission at any distance from the central star. Larger particles may need to absorb multiple photons per cooling time to reach the required temperature, confining their 10 μm emission to a region close to the central star. In order to estimate whether or not multiple photon processes play a role for PAHs of different sizes in the outer disks of HD 97048 and HD 100546, we must consider the UV flux in these stars at the distances where we observe the PAH emission. The UV flux at any distance from the central star, assuming no extinction, is given by

$$F_{\rm UV}(R) = \frac{L_{\rm UV}}{4\,\pi R^2}. \quad (1)$$

The energy absorption rate of a PAH molucule with $n_{\rm C}$ carbon atoms is given by:

$$E_{\rm abs} = \kappa\, n_{\rm C}\, F_{\rm UV} \quad (2)$$

where $\kappa = 7 \times 10^{-18}$ cm^2/C-atom (Joblin et al. 1996). Expressing Eq. (2) in convenient units, the energy absorption rate of a PAH molecule as a function of distance to the central star is given by

$$E_{\rm abs}(R) \approx 6\, n_{\rm C}\, \frac{L_{\rm UV}}{R^2} \quad \left[{\rm eV\ s^{-1}}\right] \quad (3)$$

where $L_{\rm UV}$ is the star's UV luminosity in $L_\odot$, and R the distance to the star in AU.

The temperature of a PAH molecule, after it has just absorbed a UV photon, is given by (Schutte et al. 1992):

$$T \approx 2000 \left(\frac{E_\gamma}{n_{\rm C}}\right)^{0.4} \quad [{\rm K}] \quad (4)$$

where E_γ denotes the photon energy in eV. The observed UV flux of HD 97048 is 6.50×10^{-9} erg s^{-1} cm^{-2}

Table 2. The the photon absorption rate n_γ for a typical ISM PAH molecule (at the distance from the star where the PAH emission is observed), and the minimum number of C-atoms per molecule needed for multi-photon processes to be significant ($n_{\rm min}$).

star	*FWHM* [AU]	n_γ [s^{-1}]	$n_{\rm min}$ [C-atoms]
HD 97048	110 ± 40	$0.079^{+0.116}_{-0.036}$	633^{+544}_{-377}
HD 100546	140 ± 50	$0.049^{+0.069}_{-0.022}$	1026^{+864}_{-602}

(van Kerckhoven et al. 2002), with an assumed distance of 180 pc (van den Ancker et al. 1998), this yields a UV luminosity of 2.52×10^{34} erg s^{-1}, which corresponds to 6.54 $L_\odot$. The bolometric luminosities of HD 97048 and HD 100546 are 40.7 and 36.0 $L_\odot$, respectively (van den Ancker et al. 1998). Since the spectral types of both stars (A0 and B9) are almost identical, we assume that the spectral shape of HD 100546 equals that of HD 97048, yielding a UV luminosity of $(36.0/40.7) \times 6.19 = 5.48$ $L_\odot$ for HD 100546.

The photon absorbtion rates n_γ for PAH molecules with 50 C-atoms (typical, small ISM PAH), and the minimum number of C-atoms needed to absorb 1 photon per second $n_{\rm min}$ (the cooling time of a PAH molecule is about 1 s (Bakes et al. 2001), so multi-photon processes will become significant for particles containing more than $n_{\rm min}$ carbon atoms), are given in Table 2. The median energy for a UV photon in these stars is 7.5 eV (van Kerckhoven et al. 2002).

In both stars, multi-photon processes will become important only for PAH particles containing more than about 1000 C-atoms, at the distances where the PAH emission is observed (note that extinction, which is likely present in the lines of sight from the star to the outer disk, could significantly increase this number). The temperature that such a PAH molecule attains upon absorbtion of a single 7.5 eV photon is about 280 K, which is just warm enough to emit significantly at 8 μm. Taking into account multi-photon processes, this temperature will increase somewhat. Therefore, the carrier of the 8.2 μm excess emission could either be a relatively large PAH, in which case multi-photon processes are important, or a smaller PAH consisting of less than about 500 C-atoms which is heated to some 400 K upon absorption of a single UV photon. In the former case, the 8.2 μm excess emission must be confined to regions close (<1″) to the central star, in the latter, the carrier can be excited out to larger distances.

HD 97048 provides the opportunity to constrain the nature of the carrier of the 8.2 μm excess emission, as it is surrounded by both a circumstellar disk and a remnant cloud. If the 8.2 μm excess emission is seen both in the central source (disk) and the surrounding cloud, the carrier must be relatively small, and is excited by single-photon processes. If the excess emission is seen in the central source only, the carrier could either be large (requiring multi-photon excitation) and/or be synthesized locally in the disk. Unfortunately there is no straightforward way to distinguish between the carrier of the excess emission being present both in the cloud and the disk but seen only in the disk because of the required multi-photon excitation, and the carrier being present in the disk only.

5.3. HD 97048: Disk and nebula

HD 97048 is surrounded by a reflection nebula, which has been shown to be a source PAH emission (SI01). In the previous sections we discussed the properties of the central source, which we associate with the star and its circumstellar disk. In this section we compare the disk spectrum, which we will call the "on source spectrum", with the ISO-SWS spectrum. The ISO spectrum contains both the disk emission and emission from the diffuse cloud that surrounds the system.

Comparing the two spectra (top panel of Fig. 2), we see that the peak/continuum ratio in the PAH features is different between the on-source spectrum and the ISO SWS spectrum. The ISO spectrum shows stronger PAH emission bands than the on-source spectrum. Note that we multiplied the on-source spectrum by a factor 1.08, such that the continuum level in the ISO and TIMMI 2 spectra match, faciliating comparison of the PAH peak/continuum ratios. Since the absolute photometric accuracy of both ISO-SWS and ground based spectra is about 15%, the continuum level in the two spectra is equal within errors. Moreover, the slope of the continuum emission is indistinguishable between the on-source and ISO spectrum. This again suggests that the disk is the only source of continuum radiation in the nebula. Whereas the central source shows both continuum and PAH feature emission, emission from surrounding nebula seems to be restricted to the PAH bands. Very low level continuum emission in the nebula cannot be excluded on the basis of our data, however.

An interesting possibility for the study of objects like HD 97048, is the extraction of multiple spectra along the slit. In this way, one can study the properties of the PAHs as a function of position, and possibly detect differences between the nebular PAHs and the PAH population in the disk. Unfortunately, our data are not of sufficient quality to do this, but we emphasize the potential of such studies (see also Sect. 5.2).

To account for the observed *FWHM* of the central component, as shown in Fig. 2, the physical size of the emitting region responsible for the continuum radiation cannot be significantly smaller than 100 AU. A population of very small, non-thermal equilibrium grains (VSG) must be the source of the continuum. Note that these grains cannot be silicates, since HD 97048 neither shows the strong, broad 9.7 μm emission band from small, amorphous silicates, nor the emission bands associated with crystalline silicates.

Figures 1 and 2 show that both group I stars are extended at 8.6, 11.3 and (HD 97048) 12.7 μm, corresponding to the wavelengths of the *UIR* emission bands. The red wing of the 7.7–7.9 μm *UIR* complex is observable from the ground and is spatially extended in our spectra as well. Peeters et al. (2002) show that the group of isolated HAEBE stars show similar behavior of the position and relative strength of the *UIR* bands as detected by ISO. for HD 97048 however they note that the ratio of 7.6 to 7.8 μm band strength is different from that of the other HAEBE stars. HD 97048 also differs from HD 100546 in that

the former has an extended optical reflection nebula while the latter has not.

5.4. PAH evolution

It is generally accepted that the carriers of the *UIR* emission bands are Polycyclic Aromatic Hydrocarbons (PAHs). Our results show that the *UIR* emission in HD 97048 and 100546 is extended on a scale of some 100 AU. Interestingly, this size coincides with the outer disk scale in flaring (group I) disk models. Presumably, the PAHs are localized in the flaring circumstellar disk around these sources. HD 97048 shows in addition a PAH component extended on a scale of some 1000 AU (SI01), which is likely associated with a remnant of the collapsing envelope around this source.

Recently, an extensive study of interstellar and circumstellar PAHs has revealed the presence of systematic variations in the profiles and peak positions of the main bands from source to source (Peeters et al. 2002). Specifically, the 6.2 and 7.7 μm bands are distinctly different for sources which have recently synthesized their PAHs in their ejecta (e.g., post AGB objects and planetary nebula) from those which are illuminating general interstellar medium materials. Two of the sources in this study – HD 97048 and HD 100546 – were also included in the Peeters et al. sample. The spectral characteristics of the *UIR* bands in these two sources are very different from those in sources with pure ISM materials. In particular, the 6.2 and 7.7 μm bands in the spectrum of HD 97048 are intermediate between those of of pure interstellar and pure circumstellar sources. In fact, a linear combination of these types of spectra provides a good fit to the observations of HD 97048 (van Kerckhoven et al. 2002). It is tempting to localize the PAHs with circumstellar spectral characteristics in the flaring disk while the ISM-PAHs might reside in the envelope of this source. Our data do not allow us to critically test this hypothesis, but our method may do so (see Sect. 5.3). The 6.2 and 7.7 μm bands in HD 100546 are very similar to those of circumstellar materials (Peeters et al. 2002) and presumably originate in the disk. In this view, while all the material associated with these two sources derives originally from interstellar material, the family of PAHs that made it into the disks – and that dominates the emission spectra of these two sources – has been strongly modified. Presently, there is no direct evidence to link this modification to the disk environment – in principle the modification might have occurred during the collapse phase – but we note that HD 97300 – the neighbor of HD 97048 – shows a very similar *UIR* spectrum while the PAH emission in this source is known to be extended on a scale of several 1000 AU (van Kerckhoven et al. 2002, SI01).

The processes driving the modification of PAHs around young stellar objects are not known. They might range from changes in the charge state of the emitting PAH family driven by variations in the physical conditions (e.g., illuminating FUV field or electron density), variations in the size spectrum of the PAHs driven by coagulation, chemical changes driven by the exposure to the stellar radiation field, or even a complete chemical re-formation of PAHs in these disk environment.

6. Conclusions

We have presented spatially and spectrally resolved 10 μm emission in the Herbig Ae stars HD 100546 and HD 97048 (both group I). The continuum emission outside the *UIR* bands is possibly resolved in HD 100546, whereas it is clearly extended in HD 97048, with a *FWHM* of ≈110 AU. The *UIR* emission is resolved in both stars and arises from a physically larger region than the continuum emission. HD 104237 (group II) is unresolved in our observations. Our findings are consistent with the hypothesis put forward by Meeus et al. (2001b), namely that group I sources have flaring outer disks, whereas group II sources do not. This hypothesis has recently been supported theoretically by Dullemond (2002) and Dullemond and Dominik (accepted for publication in A&A, 2004) who showed, using 2D radiative transfer modeling, that both flaring and non-flaring disks are natural and self-consistent solutions of the equations of hydrostatic equilibrium in passive, irradiated circumstellar disks.

The continuum emission in HD 100546 arises from a much smaller region than the PAH emission. The warm silicates are confined to the innermost regions of the disk. The continuum emission in HD 97048 is spatially extended on a scale of ≈100 AU. Together with the absence of the spectral signature of small silicate grains, this indicates that carbon rich very small grains are responsible for the continuum emission in the disk. Small carbonaceous particles are an important source of opacity in circumstellar disks and may dominate the opacity when no small silicate grains are present.

Our data suggest that in HD 97048, the excess emission seen around 8.2 μm, indicative of processed carbon rich material, is confined to the disk. This is possibly consistent with an ISM-type PAH contribution at scales of ≈1000 AU, and a modified PAH population at ≈100 AU. We argue that spatially resolved longs-lit spectroscopy using large telescopes on good 10 μm sites has strong potential for the study of (differential) dust evolution in the outer disks of HAe stars, and – if present – their surrounding cloud remnant.

Acknowledgements. We would like to thank the TIMMI 2 team for excellent assistance during the observations. Miska Le Louarn and Marc Sarazin are acknowledged for clarifying discussions on atmospheric turbulence.

References

Aitken, D. K., & Roche, P. F. 1981, MNRAS, 196, 39
Augereau, J. C., Lagrange, A. M., Mouillet, D., & Ménard, F. 2001, A&A, 365, 78
Bakes, E. L. O., Tielens, A. G. G. M., & Bauschlicher, C. W. 2001, ApJ, 556, 501
Bouwman, J., de Koter, A., Dominik, C., & Waters, L. B. F. M. 2003, A&A, 401, 577
Chiang, E. I., & Goldreich, P. 1997, ApJ, 490, 368
Conan, R., Le Louarn, M., Braud, J., Fedrigo, E., & Hubin, N. N. 2003, in Future Giant Telescopes, ed. J. Angel, P. Roger, & R. Gilmozzi, Proc. SPIE, 4840, 393
Danks, A., Vieira, G., Grady, C., et al. 2001, Am. Astron. Soc. Meet., 199, 6014
Dullemond, C. P. 2002, A&A, 395, 853

Dullemond, C. P., Dominik, C., & Natta, A. 2001, ApJ, 560, 957
Eisner, J. A., Lane, B. F., Akeson, R. L., Hillenbrand, L. A., & Sargent, A. I. 2003, ApJ, 588, 360
Fisher, R. S., Telesco, C. M., Piña, R. K., Knacke, R. F., & Wyatt, M. C. 2000, ApJ, 532, L141
Gürtler, J., Schreyer, K., Henning, T., Lemke, D., & Pfau, W. 1999, A&A, 346, 205
Grady, C. A., Polomski, E. F., Henning, T., et al. 2001, AJ, 122, 3396
Herbig, G. H. 1960, ApJS, 4, 337
Jayawardhana, R., Fisher, R. S., Telesco, C. M., et al. 2001, AJ, 122, 2047
Joblin, C., Tielens, A. G. G. M., Allamandola, L. J., & Geballe, T. R. 1996, ApJ, 458, 610
Liu, W. M., Hinz, P. M., Meyer, M. R., et al. 2003, ApJ, 598, L111
Mannings, V., & Sargent, A. I. 1997, ApJ, 490, 792
Meeus, G., Waters, L. B. F. M., Bouwman, J., et al. 2001a, A&A, 365, 476
Meeus, G., Waters, L. B. F. M., Bouwman, J., et al. 2001b, A&A, 365, 476
Millan-Gabet, R., Schloerb, F. P., & Traub, W. A. 2001, ApJ, 546, 358
Natta, A., Prusti, T., Neri, R., et al. 2001, A&A, 371, 186
Pantin, E., Waelkens, C., & Lagage, P. O. 2000, A&A, 361, L9
Peeters, E., Hony, S., van Kerckhoven, C., et al. 2002, A&A, 390, 1089
Prusti, T., Natta, A., & Palla, F. 1994, A&A, 292, 593
Reimann, H., Weinert, U., & Wagner, S. 1998, in Infrared Astronomical Instrumentation, ed. A. M. Fowler, Proc. SPIE, 3354, 865
Ressler, M. E., & Barsony, M. 2003, ApJ, 584, 832
Sandrock, S., Amestica, R., Duhoux, P., Navarrete, J., & Sarazin, M. S. 2000, in Advanced Telescope and Instrumentation Control Software, ed. H. Lewis, Proc. SPIE, 4009, 338
Schutte, W. A., Tielens, A. G. G. M., & Allamandola, L. J. 1992, in Astrochemistry of Cosmic Phenomena, IAU Symp., 150, 137
Siebenmorgen, R., Prusti, T., Natta, A., & Müller, T. G. 2000, A&A, 361, 258
Skinner, S. L., Brown, A., & Stewart, R. T. 1993, ApJS, 87, 217
van den Ancker, M. E., de Winter, D., & Tjin A Djie, H. R. E. 1998, A&A, 330, 145
van Kerckhoven, C., Tielens, A. G. G. M., & Waelkens, C. 2002, A&A, 384, 568
Waelkens, C., Waters, L. B. F. M., de Graauw, M. S., et al. 1996, A&A, 315, L245